

ОБЪЕДИНЕННЫЙ  
ИНСТИТУТ  
ЯДЕРНЫХ  
ИССЛЕДОВАНИЙ  
ДУБНА



9/VI-75

E1 - 8694

S-67

2089/2-75

B.Śłowiński, Z.Strugalski, B.Średniawa

BACKWARD PROTON EMISSION  
FROM THE REACTION  $\pi^+ + \text{Xe}$   
AT 2.34 GEV/C

**1975**

E1 - 8694

B.Słowiński, Z.Strugalski, B.Średniawa

**BACKWARD PROTON EMISSION  
FROM THE REACTION  $\pi^+ + \text{Xe}$   
AT 2.34 GEV/C**

Submitted to ЯФ

Объединенный институт  
ядерных исследований  
БИБЛИОТЕКА

## INTRODUCTION

In this paper we present the results of investigation of the angular and energy distributions of protons from the reaction  $\pi^+ + \text{Xe}$  at 2.34 GeV/c, in which at most four charged secondary particles are observed.

Previously <sup>/1-3/</sup> we have found that the interactions of fast pions with Xe -nuclei, in which a small number  $N_{\text{ch}}$  of charged secondary particles is observed, do not differ from the corresponding interactions of free nucleons with respect to the characteristics of  $\pi$  -mesons produced in these interactions. Taking into account simple model assumptions we estimated that half of these interactions occur for the values of impact parameter  $\geq 0.8R$ , where  $R$  is the radius of the target nucleus <sup>/3/</sup>.

However, in this so-called class of quasidelementary interactions about 1/3 of protons were observed to be emitted at angles greater than  $90^\circ$  in the laboratory (L) frame <sup>/4/</sup>, which was not observed in collisions with free nucleons.

The characteristics of protons emitted backwards in L are of great interest from the point of view of cumulative particle emission <sup>/5/</sup> and of nuclear scaling <sup>/6/</sup>. Important information concerning the nuclear surface can also be drawn from these characteristics. In the present paper use was made of the photographs obtained in an exposure of the  $^{26}\ell$  xenon bubble chamber to a  $\pi^+$  beam of 2.34 GeV/c.

## METHOD OF INVESTIGATION

Out of 50 000 scanned photographs from the xenon bubble chamber, 2358 events of  $\pi^+ - \text{Xe}$  interaction were chosen, in which no more than four tracks of charged

secondary particles and an arbitrary number  $N_\gamma$  of gamma quanta were observed. In each event, in which secondary interactions were not observed, the emission angles and ranges of charged secondary particles were measured. These particles were further counted as protons. The contamination of  $\pi^-$  -mesons did not exceed a few per cent. Deuterons among the registered secondary particles were not identified. The minimum value of the path length amounts to 8.5 mm. This corresponds to the proton kinetic energy  $E_k = 30 \text{ MeV}$  <sup>/7/</sup>. The maximum value of the kinetic energy of protons, which stop in the bubble chamber, is equal to 260 MeV. It should be remarked that for protons with  $E_k \leq 170 \text{ MeV}$  the chamber is a detector of  $4\pi$  -geometry.

A relative error in measuring the proton energy did not exceed 2 per cent, the error in determining the angle of secondary particles was not greater than 5 degrees. The statistical weight, which is due to the geometric shape of the chamber was ascribed to each registered track of the charged particle stopping inside the chamber.

Table 1

The numbers of events in  $\pi^+$ -Xe interactions at 2.34 GeV/c in which the number  $N_{ch}$  of charged secondary particles and the number  $N_p$  of protons with  $E_k = 30-250 \text{ MeV}$  stopping in the chamber are registered

$k$	$N_{ch}$	0	1	2	3	4	all
0		8	311	354	285	128	1086
1		-	38	287	303	153	781
2		-	-	31	179	160	370
3		-	-	-	22	93	115
4		-	-	-	-	6	6
all		8	349	672	789	540	2358

We estimated maximal statistical weights connected with losing the tracks caused by their mutual superposition and also with losing tracks of particles emitted at small angles with respect to the optical radii passing from the point of interaction to the objective of the camera. For protons of kinetic energy  $E_k \geq 30 \text{ MeV}$  these values do not exceed 1.1. The maximal statistical weight of the proton track connected with its secondary interaction does not exceed 1.2.

Table 1 gives the numbers of selected  $\pi^+$  - Xe interactions corresponding to different numbers  $N_{ch}$  and numbers  $N_p$  of protons which stop in the chamber.

## EXPERIMENTAL RESULTS

Below the angular and energy distributions in L for different intervals of emission angles and for different emission multiplicities of protons emitted in  $\pi^+$  - Xe interactions are given, in which no more than four charged secondary particles are observed.

### 1. Angular and energy distributions

Fig. 1 shows the distributions of protons against the emission angle in L for different multiplicities  $k$  of emitted protons in the reaction  $\pi^+ + \text{Xe} = k p + \text{anything}$  ( $k=1,2,3,4$ ) at 2.34 GeV/c. In this figure is also plotted the angular distribution from the reaction  $\pi^+ + p \rightarrow p + \text{anything}$  at 2.34 GeV/c <sup>/8/</sup> using the material kindly delivered to us by Dr. Shafranov. From this figure the conclusion can be drawn that the quoted distributions of protons from the reaction  $\pi^+ + \text{Xe} \rightarrow k p + \text{anything}$  at 2.34 GeV/c do not depend on  $k$  withing experimental errors and essentially differ from the corresponding proton distributions from the reaction  $\pi^+ + p$  at 2.34 GeV/c.

But it should be stressed that the ratio F/B of the frequency of forward emission to that of backward emission (in L) decreases with increasing number  $k$  (see table 2).

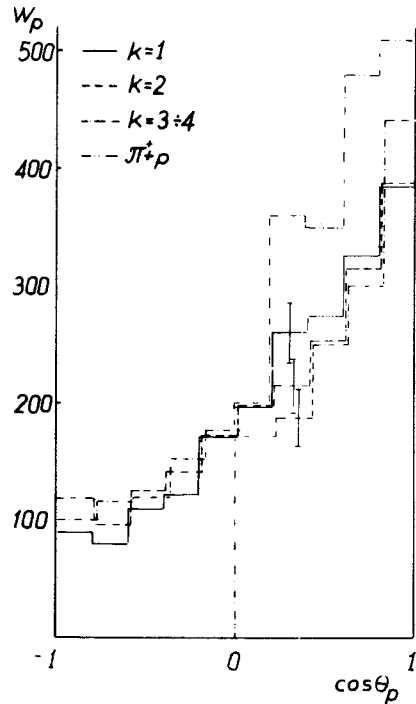


Fig. 1. Angular distributions of protons from the reaction  $\pi^+ + \text{Xe} \rightarrow kp + \text{anything}$  at 2.34 GeV/c, in which no more than four charged secondary particles are observed. These distributions correspond to different numbers  $k$  of emitted protons, the distribution of recoil protons from the reaction  $\pi^+ p$  at 2.34 GeV/c being attached <sup>/8/</sup>. The distributions are mutually normalized.

Table 2 also contains the values of mean proton kinetic energy  $\bar{E}_k$  in L and the values of the dispersion of the proton distribution for different classes of the number  $k$ . We remark that only interactions with  $N_{\text{ch}} \leq 4$  were taken into account. These data imply that the values of mean proton kinetic energy  $\bar{E}_k$  do not depend on the multiplicity of their emission and are approximately equal to half of the pion mass. This confirms our earlier results concerning all  $\pi^+ - \text{Xe}$  interactions for different numbers  $N_{\text{ch}}$  of charged particles <sup>/9/</sup>.

Table 2

The values of the ratio  $F/B$  for proton emission from the reaction  $\pi^+ + \text{Xe} = kp + \text{anything}$  at 2.34 GeV/c.  $\bar{E}_k$  is the average value of the proton kinetic energy in L,  $\sigma_{E_k}$  is the dispersion of the distribution of protons according to  $E_k$ . The number of charged secondary particles does not exceed four

k	1	2	3-4	all
$F/B$	$2.5 \pm 0.1$	$2.1 \pm 0.1$	$2.0 \pm 0.1$	$2.3 \pm 0.1$
$\bar{E}_k$ (MeV)	$75.4 \pm 0.7$	$78.1 \pm 0.8$	$76.3 \pm 0.6$	$77.1 \pm 0.7$
$\sigma_{E_k}$ (MeV)	32	33	29	32

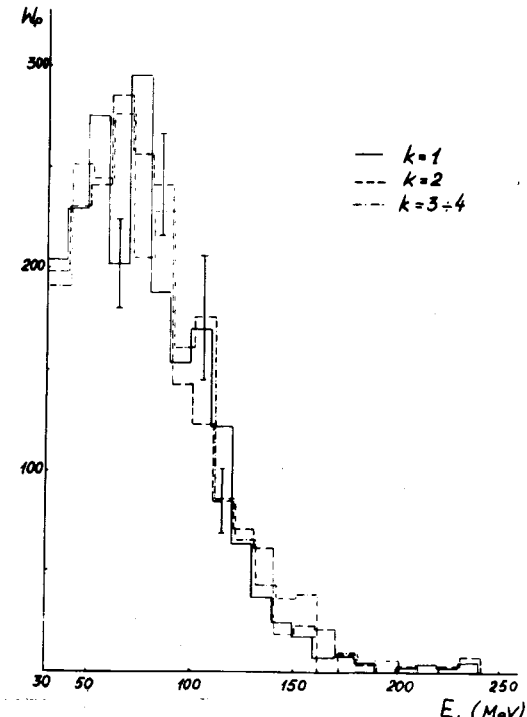


Fig. 2. Energy distributions of protons from the reaction  $\pi^+ + \text{Xe} \rightarrow kp + \text{anything}$  at 2.34 GeV/c, in which no more than four charged secondary particles are observed. These distributions correspond to different numbers  $k$  of emitted protons. The distributions are mutually normalized.

As it follows from Fig. 2, where the energy distributions of protons for the classes of interaction with different  $k$  values are plotted, and from Table 2, the shape of these distributions does not depend, within errors, on the number of emitted protons.

Fig. 3 presents the energy distributions of protons from all classes of interactions for all  $k$ . In the

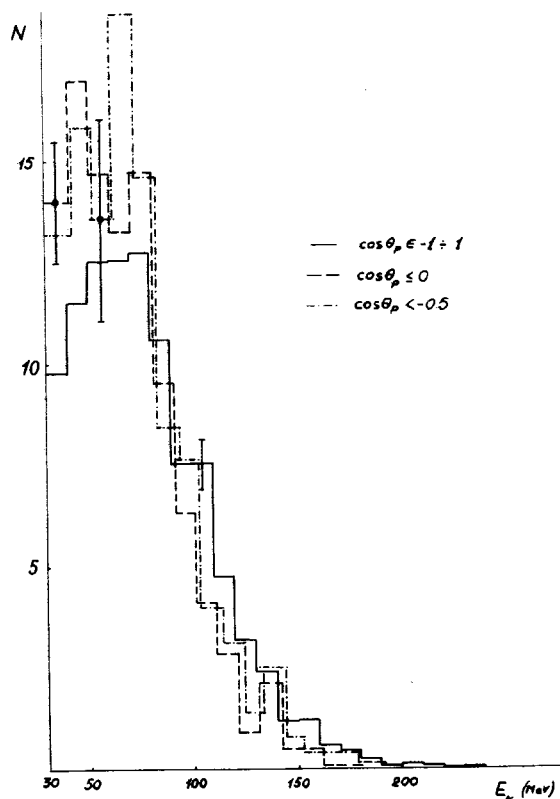


Fig. 3. Energy distributions of protons from the reaction  $\pi^+ + \text{Xe} \rightarrow kp + \text{anything}$  at 2.34 GeV/c, in which no more than four charged secondary particles are observed. The mutually normalized distributions correspond to different intervals of proton emission angles.

same figure are also plotted the energy distributions of protons, for which  $\cos \theta_p \leq 0$  and  $\cos \theta_p \leq -0.5$  respectively ( $\theta_p$  is the emission angle of the proton). The distributions are mutually normalized. We can remark that the energy distributions of backwards emitted protons do not show a perceptible dependence on the proton emission angle and differ from the energy distributions of forwards emitted angles.

## 2. Lorentz Invariant Cross Section

The Lorentz invariant cross section (LICS)  $\rho(E_k)$  has been calculated as follows

$$\rho(E_k) = \frac{2E_t}{\sigma_{in}} \frac{d^3\sigma}{dp^3} \approx \frac{2}{\sigma_{in}} \frac{r}{P} \bar{\sigma}_{1 \text{ prot}} w_P [(\text{GeV}/c)^{-2}c], \quad (1)$$

where  $E_t$  is the total proton energy in L,  $\bar{\sigma}_{1 \text{ prot}}$  is the mean cross section for emission of one proton in the investigated region,  $\bar{\sigma}_{1 \text{ prot}} = (0.194 \pm 0.019)$  mb;  $\sigma_{in}$  is the total cross section for inelastic  $\pi^+ - \text{Xe}$  interactions at 2.34 GeV/c,  $\sigma_{in} = (1238 \pm 30)$  mb<sup>3/</sup>,  $w_P$  is the sum of statistical weights of protons emitted in the interval of proton kinetic energy  $\Delta E_k = 20$  MeV and in the given interval of emission angles; the coefficient  $r = 10$  for the distributions with the intervals of emission angles  $\Delta \cos \theta_p = -0.2$  and  $r=2$  for the distributions of protons emitted backwards ( $\cos \theta_p < 0$ ).

In Fig. 4 the values of LICS  $\rho(E_k)$  of proton emission from all  $\pi^+ - \text{Xe}$  interactions for all values of  $k$  corresponding to five different intervals of emission of protons emitted backwards in L are plotted as a function of proton kinetic energy in L. The corresponding numerical data are given in Table 3.

From these data the conclusion can be drawn that the LICS of backward proton emission does not show, within the achieved experimental accuracy any dependence on the emission angle. Fig. 5 presents the values of the function  $\rho(E_k)$  corresponding to protons emitted backwards,

Table 3

LICS  $\rho(E_k)$  for protons emitted in different angular intervals into the backward hemisphere in  $L$  in the reaction  $\pi^+ + Xe \rightarrow p + \text{anything}$  at 2.34 GeV/c. The number of charged secondary particles  $N_{cb} < 4$ .  $\cos\theta_p$  is the cosine of the proton emission angle in  $L$ ,  $E_k$  is the proton kinetic energy in  $L$ .

$\cos\theta_p$	-1+-.8	-.8+-.6	-.6+-.4	-.4+-.2	-.2+0	$\leq 0$
$E_k$ (MeV)						
30-50	1.69±0.356	1.517±0.334	2.275±0.429	2.158±0.415	3.383±0.558	2.205±0.273
50-70	1.658±0.326	1.042±0.245	1.365±0.289	1.630±0.322	2.360±0.409	1.611±0.203
70-90	0.947±0.218	0.865±0.207	1.110±0.240	1.531±0.293	1.580±0.299	1.207±0.156
90-100	0.341±0.116	0.516±0.146	0.385±0.124	0.458±0.137	0.625±0.163	0.465±0.074
110-130	0.145±0.071	0.112±0.062	0.172±0.077	0.221±0.088	0.108±0.060	0.152±0.035
130-150	0.030±0.030	0.091±0.053	0.182±0.076	0.055±0.041	0.125±0.063	0.097±0.026
150-170	-	0.057±0.041	-	0.059±0.041	-	0.023±0.012
170-190	-	0.027±0.027	-	0.040±0.033	-	0.013±0.008

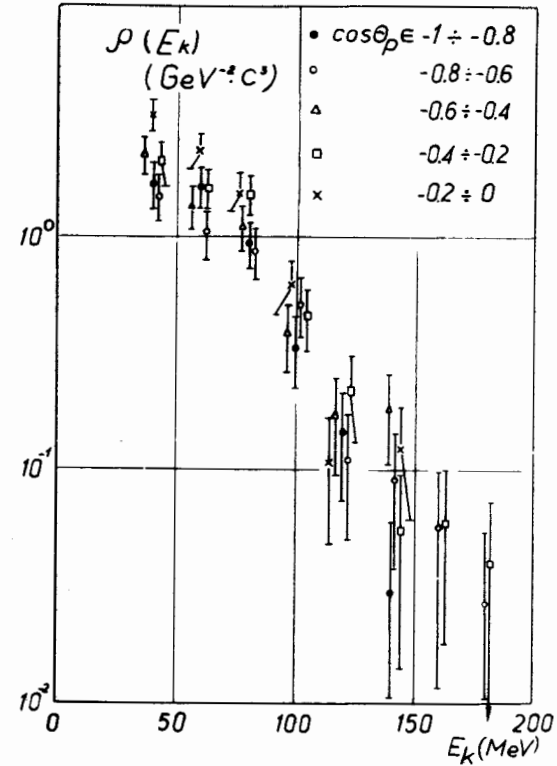


Fig. 4. Lorentz invariant cross sections (LICS) of backward proton emission in  $\pi^+ - Xe$  interactions at 2.34 GeV/c, in which no more than four charged secondary particles are observed.  $E_k$  is the proton kinetic energy in  $L$ . The cross sections correspond to different values  $E_k$  of proton kinetic energy in  $L$  and to different intervals of the cosines of proton emission angles in  $L$ .

summed over all emission angle intervals. In this figure two approximating curves of the form

$$\rho(E_k) = a \exp(-E_k/E_0) \quad (2)$$

are also plotted. If we assume that all experimentally

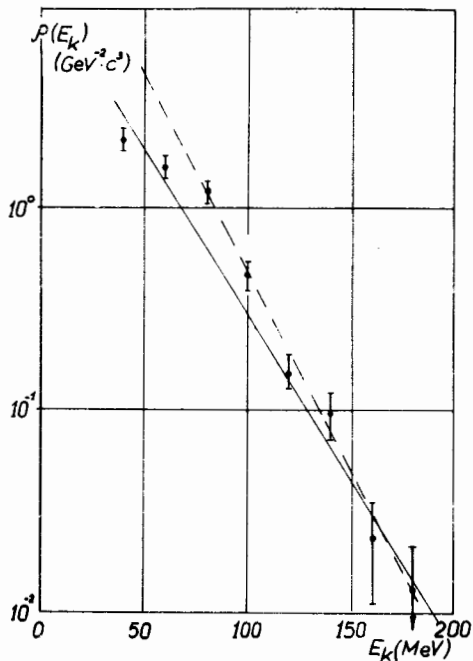


Fig. 5. LICS of backward proton emission in  $\pi^+ - \text{Xe}$  interactions at 2.34 GeV/c, in which no more than four charged secondary particles are observed.  $E_k$  is the kinetic energy of protons in L. The solid line represents the function  $\rho(E_k)$  approximating experimental values. The dashed line represents a similar function approximating all experimental values except for the two ones corresponding to minimal values of  $E_k$ .

determined values of LICS are described by the function (2), we have

$$a = (10.941 \pm 1.457) (\text{GeV}/c)^{-2} c$$

$$E_0 = (28.91 \pm 1.29) \text{ MeV},$$

and

$$\chi^2 = 23.5 \text{ at 6 degrees of freedom.}$$

If we further assume a more acceptable hypothesis that the function (2) describes correctly all the points plotted

Table 4

LIRS  $f(p^2)$  for protons emitted in different angular intervals into the backward hemisphere in L in the reaction  $\pi^+ + \text{Xe} \rightarrow p + \text{anything}$  at 2.34 GeV/c. The number of charged secondary particles  $N_{k \leq 4} \cdot \cos \theta$  is the cosine of the proton emission angle in L,  $p^2$  is the proton momentum squared in L.

$\cos \theta$	$-1 \div -0.8$	$-0.8 \div -0.6$	$-0.6 \div -0.4$	$-0.4 \div -0.2$	$-0.2 \div 0$	$\leq 0$
$p^2 (\text{GeV}/c)^2$						
0.0575-0.0925	0.152±0.033	0.140±0.031	0.202±0.039	0.180±0.036	0.269±0.047	0.167±0.024
0.0925-0.1275	0.141±0.026	0.075±0.020	0.140±0.029	0.137±0.029	0.252±0.043	0.149±0.019
0.1275-0.1675	0.097±0.020	0.092±0.022	0.100±0.023	0.194±0.027	0.156±0.030	0.116±0.015
0.1625-0.1975	0.046±0.014	0.057±0.016	0.053±0.015	0.082±0.020	0.062±0.017	0.060±0.009
0.1975-0.2375	0.027±0.010	0.028±0.010	0.021±0.009	0.039±0.012	0.039±0.012	0.031±0.006
0.2325-0.2675	0.0037±0.0033	0.0033±0.0033	0.007±0.005	0.014±0.007	0.007±0.005	0.0071±0.0022
0.2675-0.3025	0.0032±0.0032	0.0063±0.0045	0.016±0.007	-	0.010±0.006	0.0070±0.0022
0.3025-0.3375	-	0.0061±0.0043	-	0.0062±0.0043	-	0.0025±0.0012
0.3375-0.3725	-	0.0059±0.0042	-	-	-	0.0012±0.0008
0.3725-0.4075	-	-	-	0.0043±0.0035	-	0.0009±0.0008



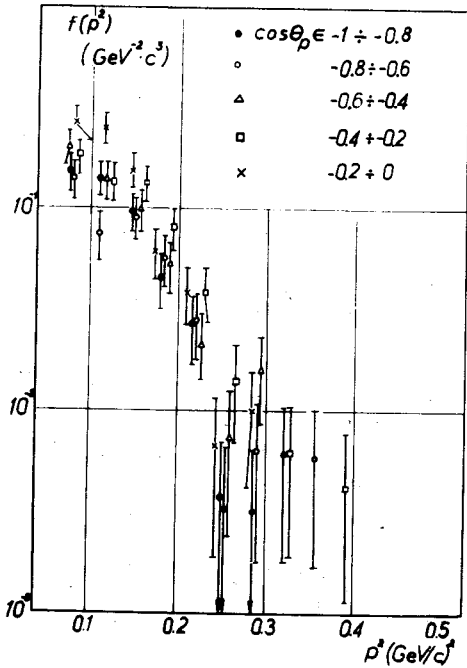


Fig. 6. The same as in Fig. 4, but versus the proton momentum squared in  $L$ .

in Fig. 5, except for those for two lowest values of  $E_k$ , we have

$$a = (5100 \pm 19.68) \text{ GeV/c}^{-2} c,$$

$$E_0 = (21.17 \pm 1.67) \text{ MeV},$$

$$\chi^2 = 1.98 \text{ at 4 degrees of freedom.}$$

Use is also made of the dependence of the LICS on the proton momentum squared in  $L^{6/}$ . Therefore we have also performed a similar analysis of our experimental data. The results of this analysis are given in Table 4 and in Figs. 6 and 7. In this case the LICS is determined by

$$f(p^2) \approx \frac{E_t}{p} \frac{\bar{\sigma}_{l \text{ prot}}}{\sigma_{in}} r W_p \quad [(\text{GeV/c})^{-2} c], \quad (3)$$

where  $W_p$  is the sum of the statistical weights of protons emitted in the interval of the values of proton momentum squared in  $L$ ,  $\Delta(p^2) = 0.035 (\text{GeV/c})^2$  and in the given interval of emission angles. The experimentally obtained values of the LICS of backwards emitted protons are approximated by means of the function

$$f(p^2) = A \exp(-B p^2). \quad (4)$$

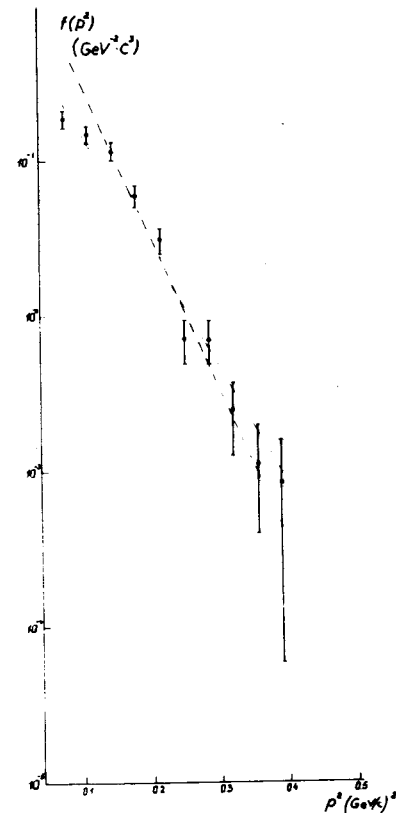


Fig. 7. The same as in Fig. 5, but versus the proton momentum squared in  $L$ . The shape of the approximating function is  $f(p^2) = A \exp(-B p^2)$ .



$E_k \geq 30$  MeV is small<sup>/10/</sup>. Such a conclusion can be regarded as a supplementary confirmation of a considerable clusterization of nucleons on the surface of the nucleus.

The dependence of the LICS of backward proton emission on their kinetic energy (or on the squared momenta), which we have obtained here, is similar to the corresponding dependence in the case of interactions at other energies as well as for other secondary particles and target nuclei<sup>/5,6/</sup>. Nevertheless, it should be remarked that for a more precise description of the shape of the LICS, in particular in the region of small values of kinetic energy (or squared momentum) of protons, a more complicated function than an exponential dependence of the type (2) (or (4)) is needed. The parameter  $E_0$  or the so-called distribution temperature of protons does not exceed 29 MeV, which is roughly two times as small as in the case of backward pion emission<sup>/5/</sup>.

The authors express their gratitude to Dr. T. Kanarek for his friendly help in performing computations.

#### References

1. Б.Словинский, З.Стругальский. Сообщение ОИЯИ, Р1-6557, Дубна, 1972.
2. Б.Словинский, З.С.Стругальский. Сообщение ОИЯИ, Р1-7439, Дубна, 1973.
3. Б.Словинский. ЯФ, 19, вып. 3, 495 /1974/.
4. Б.Словинский, З.С.Стругальский. Препринт ОИЯИ, Р1-5592, Дубна, 1971.
5. A.M. Baldin, N. Ghiordanescu, L.K. Ivanova, N.S. Moroz, A.A. Povtorejko, V.B. Radomanov, V.S. Stavinsky, V.N. Zubarev. Report JINR, E1-8054, Dubna, 1974; А.М.Балдин, В.К.Бондарев, Н.Гиорданеску, В.Н.Зубарев, Л.К.Иванова, Н.С.Мороз, А.А.Повторейко, В.Б.Радоманов, В.С.Ставинский, Ю.П.Яковлев. Препринт ОИЯИ, 1-8249, Дубна, 1974.
6. А.В.Арефьев, Ю.Д.Баюков, В.Б.Гаврилов, В.И.Ефременко, Ю.М.Зайцев, Т.А.Лексин, Д.А.Сучков. Письма в ЖЭТФ, 20, вып. 8, 585 /1974/.

7. Т.Канарек, З.С.Стругальский. Препринт ОИЯИ, 1-3320, Дубна, 1967.
8. Н.Ангелов, И.М.Граменицкий, Х.Каназирски, П.Керачев, Р.Ледницки, А.М.Моисеев, А.Прокеш, Л.А.Тихонова, А.Б.Фенюк, М.Христов, М.Д.Шафранов. Сообщение ОИЯИ, Р1-4611, Дубна, 1969.
9. Б.Словинский, З.С.Стругальский. Препринт ОИЯИ, Р1-5592, Дубна, 1971.
10. В.С.Барашенков, В.Д.Тонеев. Взаимодействия высокоэнергетических частиц и атомных ядер с ядрами. Москва, Атомиздат, 1972.

Received by Publishing Department  
on March 17, 1975.